Published online 11 May 2017

Nucleic Acids Research, 2017, Vol. 45, No. 12 ***7441–7454***
doi: 10.1093/nar/gkx405

Protein-only RNase P function in *Escherichia coli*: viability, processing defects and differences between PRORP isoenzymes

Markus Gößringer[1], Marcus Lechner[1], Nadia Brillante[2], Christoph Weber[2], Walter Rossmanith[2] and Roland K. Hartmann[1,*]

[1]Institute of Pharmaceutical Chemistry, Philipps-University Marburg, Marbacher Weg 6, 35037 Marburg, Germany and [2]Center for Anatomy & Cell Biology, Medical University of Vienna, Währinger Straße 13, 1090 Vienna, Austria

Received April 07, 2017; Revised April 26, 2017; Editorial Decision April 27, 2017; Accepted May 02, 2017

ABSTRACT

The RNase P family comprises structurally diverse endoribonucleases ranging from complex ribonucleoproteins to single polypeptides. We show that the organellar (*At*PRORP1) and the two nuclear (*At*PRORP2,3) single-polypeptide RNase P isoenzymes from *Arabidopsis thaliana* confer viability to *Escherichia coli* cells with a lethal knockdown of its endogenous RNA-based RNase P. RNA-Seq revealed that *At*PRORP1, compared with bacterial RNase P or *At*PRORP3, cleaves several precursor tRNAs (pre-tRNAs) aberrantly in *E. coli*. Aberrant cleavage by *At*PRORP1 was mainly observed for pre-tRNAs that can form short acceptor-stem extensions involving G:C base pairs, including $tRNA^{Asp}$(GUC), $tRNA^{Ser}$(CGA) and $tRNA^{His}$. However, both *At*PRORP1 and 3 were defective in processing of *E. coli* pre-$tRNA^{Sec}$ carrying an acceptor stem expanded by three G:C base pairs. Instead, pre-$tRNA^{Sec}$ was degraded, suggesting that $tRNA^{Sec}$ is dispensable for *E. coli* under laboratory conditions. *At*PRORP1, 2 and 3 are also essentially unable to process the primary transcript of 4.5S RNA, a hairpin-like non-tRNA substrate processed by *E. coli* RNase P, indicating that PRORP enzymes have a narrower, more tRNA-centric substrate spectrum than bacterial RNA-based RNase P enzymes. The cells' viability also suggests that the essential function of the signal recognition particle can be maintained with a 5′-extended 4.5S RNA.

INTRODUCTION

RNase P is the endoribonuclease responsible for the 5′-end maturation of tRNA primary transcripts (1–4). While bacterial RNase P is composed of a catalytic RNA subunit and a single protein cofactor (5), the nuclear enzyme of several major eukaryal groups (metazoans, fungi) has evolved into a complex ribonucleoprotein consisting of an RNA subunit plus up to 10 protein subunits (6,7). Until recently, the presence of a catalytic RNA subunit was thought to be the hallmark of all RNase P enzymes. The first exception from this assumption was reported in 2008 when the human mitochondrial activity was found to consist of three protein subunits and to lack an RNA component (8). Homologs of the endonuclease protein subunit of human mitochondrial RNase P, originally termed MRPP3, were identified also in distant eukaryal groups, such as land plants and kinetoplastida (9). This led to the characterization of three homologs to human MRPP3 in the land plant *Arabidopsis thaliana*, all of which were demonstrated to be genuine RNase P enzymes that are active as single polypeptides (9,10). One of the *A. thaliana* RNase P isoenzymes (termed PRORP1 for proteinaceous RNase P 1), which localizes to the mitochondria and chloroplasts, was demonstrated to sustain growth of an *Escherichia coli* mutant strain with an otherwise lethal depletion of its endogenous ribonucleoprotein RNase P (9). The two other isoenzymes *At*PRORP2 and 3 are found in the nucleus (9). Two PRORP isoenzymes also have RNase P function in the protist *Trypanosoma brucei* (*Tb*PRORP1 and 2) (11). Recently, the different PRORPs from *A. thaliana* and *T. brucei* were shown to be able to replace the nuclear RNase P ribonucleoprotein complex in yeast (11,12). An in-depth characterization of *At*PRORP3-dependent yeast strains moreover showed that the RNase P replacement did not compromise the fitness of these cells (12). Overall, these findings lead to the conclusion that protein-based RNase P enzymes are capable of carrying out the basic functions of an RNA-containing RNase P enzyme in Bacteria and Eukarya, but they raise the question why so many organisms have retained a ribonucleoprotein (RNP) RNase P enzyme.

*To whom correspondence should be addressed. Tel: +49 6421 28 25827; Fax: +49 6421 28 25854; Email: roland.hartmann@staff.uni-marburg.de

The capability to substitute for *E. coli* RNase P *in vivo* was extended here to the nuclear isoenzymes (*At*PRORP2 and 3) from *A. thaliana*. This was motivated by the idea that their complementation capacity in the *E. coli* host may differ from that of the organellar enzyme (*At*PRORP1), as (i) the latter has to act on a different set of substrates in a different cellular environment relative to the nuclear isoenzymes, (ii) recent evidence suggested differences in cleavage fidelity compared to *At*PRORP2 and 3 (13) and (iii) *At*PRORP1-dependent yeast strains grew slower than *At*PRORP2- or 3-dependent ones (12). Principally, all three *At*PRORP variants supported growth of a conditional *E. coli* RNase P mutant strain under non-permissive conditions, demonstrating their capacity to maintain basic tRNA 5′-end maturation functions in the bacterial host. Yet, relative to bacteria complemented with a plasmid encoding the homologous RNase P RNA (*rnpB*) gene, plasmid-borne expression of PRORP enzymes gave rise to bacterial growth that was impaired to an extent depending on the nature of the individual *At*PRORP variant. Determination of the 5′-cleavage sites of tRNAs in *At*PRORP1 and *At*PRORP3-complemented strains by RNA-Seq revealed increased levels of aberrant cleavage primarily in *At*PRORP1-complemented cells, which correlated with the potential of precursor tRNAs to form extended acceptor stems. Further, the processing defects of *At*PRORP enzymes were verified in biochemical studies using selected *E. coli* RNase P substrates. We observed (i) a lack of 5′-end maturation of 4.5S RNA (an RNase P substrate involved in co-translational targeting of membrane and secretory proteins) in *E. coli* cells depending on *At*PRORP1 or 3, (ii) ∼50% inaccurate 5′-end maturation of $tRNA^{His}$ by *At*PRORP1, but not *At*PRORP2 or 3, (iii) essentially no 5′-end maturation, but degradation of pre-$tRNA^{Sec}$, (iv) aberrant 5′-processing of pre-$tRNA^{Asp}$(GUC) and pre-$tRNA^{Ser}$(CGA) by *At*PRORP1 but not *At*PRORP3.

MATERIALS AND METHODS

Bacterial strains and complementation studies

Expression of the *rnpB* gene (encoding the RNase P RNA subunit) in *E. coli* strain BW strictly depends on arabinose supplementation (14). In the absence of arabinose and the presence of glucose the chromosomal *rnpB* expression in strain BW is repressed and survival of the cells depends on plasmid-encoded RNase P activities. For *in vivo* studies, the different pDG148-based expression vectors (Supplementary Table S1) were introduced into *E. coli* BW cells by electroporation. The genotypes of the strains used here are specified in Supplementary Table S2 and more methodological details are provided in the Supplementary Material.

RNA-Seq—Illumina sequencing and data evaluation

For the RNA-Seq analysis presented in Figure 3, single colonies of BW[pEc*rnpB*], BW[pAt*PRORP1*] or BW[pAt*PRORP3*] bacteria (three biological replicates of each strain) picked from agarose plates were used to inoculate 3 ml LB medium supplemented with 10 mM arabinose. After 8 h of growth at 37°C/200 rpm, cells from such pre-cultures were transferred into 50 ml fresh LB medium supplemented with 10 mM glucose to a starting OD_{600} of 0.01. Cultures were grown for 14 h at 37°C/200 rpm into stationary phase. Cells were then transferred into 200 ml of fresh glucose-containing LB medium (starting $OD_{600} = 0.1$) to initiate exponential growth. At $OD_{600} \sim 1.0$ (= outgrowth phase), cells were harvested and total RNA was prepared according to Method 1 ('Extracting RNA three times with hot phenol') described by Damm *et al.* (15). Library generation was performed at vertis Biotechnologie AG (Freising-Weihenstephan, Germany). Total RNAs were depleted of rRNA using the Ribo-Zero rRNA Removal Kit for bacteria (Epicenter). The fraction of small RNAs (<200 nt) was separated using the RNeasy MinElute Cleanup Kit (Qiagen). Oligonucleotide adapters were ligated to the 5′- and 3′-ends. First-strand cDNA synthesis was performed using M-MLV reverse transcriptase and the 3′-adapter as primer. The resulting cDNAs were PCR-amplified using a high-fidelity DNA polymerase. The cDNA was purified using the Agencourt AMPure XP kit (Beckman Coulter Genomics). The 3′- and 5′-adapters and the primers used for PCR amplification were designed for TruSeq sequencing according to the instructions of Illumina. The cDNA pool was sequenced on an Illumina NextSeq 500 system with a read length of 75 nt.

Details regarding the preparation of the initial RNA-Seq analysis that led to the detection of the 4.5S RNA processing defect in BW[At*PRORP1*] bacteria can be found in the Supplementary Material.

Reads were processed in two steps. First, nucleotides with a read quality lower than Q30 were trimmed from the end of the sequence using the FASTX Toolkit. Then homo-polymeric sequences (≥12 identical nucleotides) were trimmed using custom scripts. Mapping to *E. coli* str. K-12 substr. MG1655 (GenBank CP012868.1) was done using segemehl (16) with an *e*-value of 0.01 and a minimal read length of 10 nt. The overall statistics of the three biological replicate libraries for each strain can be found in the Supplementary Table S3.

For the data presentation in Figure 3, only tRNA reads with their 5′-end mapping to position –2, –1 or +1 (according to the *RefSeq* annotation GenBank CP012868.1) and with a minimal number of 10 reads (sum of reads corresponding to 5′-ends at –2, –1 and +1) of the respective tRNA in at least two of the biological replicates were included in the evaluation. Reads starting further upstream than position –2 are shown in the alignments of the Online Supplement (Results, 'Categorized mapping alignments for all replicates') but were not considered further. Reads starting at the 5′-end position +1 were classified as 'canonically cleaved' and reads starting at –2 or –1 were classified as 'miscleaved'. Note that bacterial $tRNA^{His}$ and $tRNA^{Sec}$ are naturally 'miscleaved' between nt –2/–1. For each tRNA meeting the aforementioned criteria, the canonically cleaved percentage of cDNA reads (5′-end at position +1) was plotted according to the equation $(\frac{N_{+1}}{N_{-2}+N_{-1}+N_{+1}}) \times 100\%$, where N_{-2}, N_{-1} and N_{+1} correspond to the number of tRNA-specific cDNA reads starting at the 5′-end position –2,

–1 and +1, respectively. Two falsely annotated $tRNA^{Met}$ molecules were assigned as $tRNA^{Ile2}$ (17). We furthermore merged sequences with identical tRNA bodies and identical nucleotides at position –1 and –2. Details can be found in the Online Supplement (http://bioinf.pharmazie.uni-marburg.de/supplements/prorp_2017/) under 'Sequences'.

Whenever reads mapped to multiple tRNAs we applied the abundance factors reported by Dong *et al.* (18). Here, we adjusted the molar ratios to our growth rates of ∼2. Hence, we averaged the values given by Dong *et al.* (18) for growth rates of 1.6 and 2.5. In cases where tRNAs were not differentiated there, we distributed the reads proportionally. For example, the number of mature tRNA reads mapping to both, $tRNA^{Gln}$(UUG) 1/2 and $tRNA^{Gln}$(UUG) 2/2, were assigned to each tRNA after multiplying with 0.5. The scores can be viewed in the respective alignments in the Online Supplement (Results, 'Categorized mapping alignments for all replicates'), which also includes the raw and scored read numbers. While this consideration of multimap reads is technically necessary for obtaining an unbiased picture, the influence of these adjustments to the processing fractions (next paragraph) was marginal and did not change the overall picture.

For details on cell growth, plasmid preparations for *in vivo* studies, the initial RNA-Seq analysis, primer extension, Western blotting, northern blot analysis (for the used probes, see Supplementary Table S4) and *in vitro* RNase P cleavage assays (conducted essentially as described (19)), see the Supplementary Material.

RESULTS

Complementation of *E. coli* RNase P RNA deficiency by *At*PRORP1, 2 and 3

We compared the organellar *At*PRORP1 isoenzyme and the nuclear isoenzymes *At*PRORP2 and 3 with respect to their ability to functionally replace *E. coli* RNase P *in vivo* (for similarity of the three PRORP isoenzymes, see Supplementary Figure S1A and B). In the test strain BW, a derivative of *E. coli* MG1655 (Supplementary Table S2), the endogenous RNase P RNA gene (*rnpB*) is expressed from a chromosome-borne P_{BAD} promoter in the presence of the inducer arabinose, whereas expression is silenced when cells grow in the presence of glucose as the carbon source. As a result, RNase P RNA is depleted (Supplementary Figure S2A) and cells stop dividing (14). Bacteria expressing *At*PRORP1 and 3 were able to rescue growth at 37°C under non-permissive conditions on LB-glucose plates (Supplementary Figure S2B). In contrast, bacteria expressing *At*PRORP2 or harboring an empty plasmid failed to rescue growth under these standard growth conditions. We previously observed that recombinant *At*PRORP2 is inactive in precursor tRNA (pre-tRNA) processing assays at 37°C, but displays vivid activity at 28°C (19). In line with this finding, *At*PRORP2 was able to sustain growth of BW bacteria in the absence of arabinose at 28°C (Supplementary Figure S2B). These findings demonstrate that all three PRORP isoenzymes from *A. thaliana* can execute tRNA 5′-end maturation to an extent that permits *E. coli* cell proliferation, consistent with their similar overall structure (Supplementary Figure S1C).

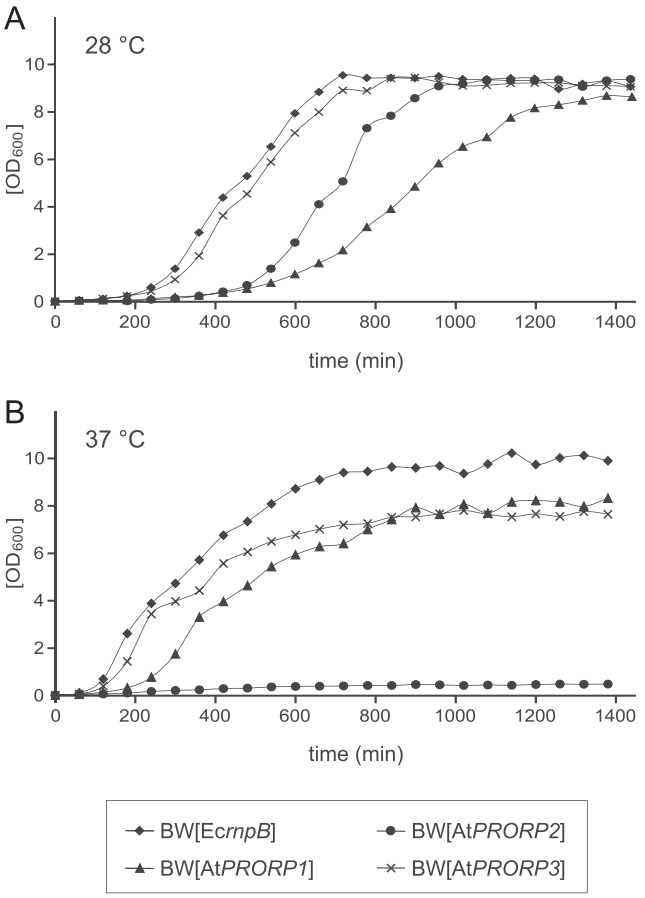

Figure 1. Growth curves of *E. coli* strains BW[Ec*rnpB*], BW[At*PRORP1*], BW[At*PRORP2*] and BW[At*PRORP3*]. Cultures were grown in the absence of arabinose in 70 ml glucose-containing LB medium at (**A**) 28°C or (**B**) 37°C with 200 rpm agitation and the OD_{600} of samples determined every 45 min. The relative growth phenotypes were reproducibly observed in four independent experiments. For generation times, see Supplementary Table S5.

Growth properties of *At*PRORP-depending *E. coli* cells

To examine how efficiently the *At*PRORP isoenzymes fulfill their RNase P function in the *E. coli* host, growth of the *At*PRORP-dependent BW bacteria in liquid medium was monitored (Figure 1). At 28°C (Figure 1A), all three *At*PRORP isoenzymes supported growth of *E. coli* BW bacteria under non-permissive conditions, reaching comparable cell densities in stationary phase. The growth behavior of the strain harboring the expression vector for *At*PRORP3 (BW[pAt*PRORP3*]) was almost identical to that of BW cells harboring the plasmid-encoded *E. coli* P RNA gene (BW[pEc*rnpB*]). However, cells depending on the RNase P activity of *At*PRORP2, or *At*PRORP1 in particular, had an extended lag phase before entering exponential growth (Figure 1A; for generation times, see Supplementary Table S5). When growth in liquid culture was monitored at 37°C, *At*PRORP2 was unable to sustain growth of BW cells (Figure 1B), in line with the failure to

grow on agar plates (Supplementary Figure S2B). Again, bacteria expressing *At*PRORP3 reproducibly showed a faster transition from lag to exponential phase than those depending on *At*PRORP1, and strains BW[At*PRORP1*] and BW[At*PRORP3*] grew to a lower final density at 37°C than BW[pEc*rnpB*] bacteria (Figure 1B). As shown by Western blot analysis, the expression levels of all three C-terminally His-tagged *At*PRORP isoenzymes were comparable in *E. coli* BW cells grown at 28°C. Likewise, expression levels of *At*PRORP1-His and *At*PRORP3-His were similar in BW cells grown at 37°C (Supplementary Figure S3). However, compared to BW cells grown at 28°C, the fraction of insoluble *At*PRORP1-His and *At*PRORP3-His fraction were increased in BW cells grown at 37°C (Supplementary Figure S3*A*, compare lanes 4 versus 12, and 8 versus 14). Thus, the quantity of functional, soluble PRORP enzymes seems to be decreased at higher growth temperatures and *E. coli* cells have to cope with larger amounts of insoluble protein. This may have contributed to the lower final density of BW[At*PRORP1*] and BW[At*PRORP3*] cultures at 37°C relative to BW[Ec*rnpB*] bacteria (Figure 1B).

RNA-Seq analysis of *At*PRORP1-depending *E. coli* cells

To detect potential processing defects in *E. coli* cells depending on PRORP, we pursued a deep sequencing (RNA-Seq) approach using total RNA from *E. coli* BW[At*PRORP1*] cells grown for 70 min under non-permissive conditions in arabinose-free medium. The relatively short period of 70 min was chosen to focus on primary effects in the transcriptome upon depletion of endogenous RNase P. The BW[At*PRORP1*] strain was chosen at the beginning of this study because it had a longer lag phase than the BW[At*PRORP3*] strain (Figure 1), thus increasing the likelihood to detect potential processing defects. As reference, we used *E. coli* MG1655, the parental wild-type strain of the BW mutant strains. *E. coli* MG1655 was considered to be equivalent to strain BW[Ec*rnpB*] (Figure 1), since both strains express *E. coli* wild type RNase P. For strains MG1655 and BW[Ec*rnpB*] we obtained very similar growth curves in LB medium supplemented with 10 mM glucose at 37°C (14), so the potentially higher gene dosage of BW[Ec*rnpB*] expressing *E. coli rnpB* from a plasmid seems not to impact on growth behavior.

A major outcome of the RNA-Seq analysis was the finding of an increased proportion of reads representing 5′-precursor 4.5S RNA (pre-4.5S RNA) in total RNA isolated from BW[At*PRORP1*] compared with MG1655 bacteria (Figure 2*A* and Supplementary Figure S4). In *E. coli*, the non-coding RNA 4.5S RNA is a verified substrate of bacterial RNase P (20,21) and plays an important role as part of the signal recognition particle that targets ribosomes to the plasma membrane (22,23).

Accumulation of pre-4.5S RNA in *At*PRORP-depending *E. coli* cells

To further validate this potential 4.5S RNA processing defect in BW[At*PRORP1*] bacteria by an independent approach, we analyzed total RNA from BW[At*PRORP1*] cells grown in arabinose-free glucose medium by primer extension using a 4.5S RNA-specific primer. Reverse transcriptase extended the 5′-^{32}P-end-labeled primer (18 nt) by 2 nt on mature 4.5S RNA. The 2-nt extension product corresponding to 5′-mature 4.5S RNA was the only signal obtained with total RNA from the parental wild type strain grown for 6 h in the presence of glucose or with RNA from BW[vector] cells (strain BW harboring the empty expression vector) grown for 6 h in the presence of arabinose (Figure 2B, lanes 1 and 3). However, primer extension using total RNA from BW[At*PRORP1*] or BW[vector] grown in the presence of glucose for the same time period resulted in much less extension product corresponding to 5′-mature 4.5S RNA and substantial amounts of longer extension products (Figure 2B, lanes 2 and 4). The identical product pattern in lanes 2 and 4 indicated that *At*PRORP1 is essentially unable to contribute to the 5′-end maturation of 4.5S RNA in the *E. coli* host.

The apparent lengths of primer extension products obtained on pre-4.5S RNA (Figure 2B, lanes 2 and 4) suggested the presence of longer precursor molecules than those reported previously (22 nt) (20). This difference to the previous study may be explained by the fact that the authors used an RNase P mutant strain (A49) under heat shock conditions, which may have caused changes in RNA processing. A search for putative promoters upstream of the 4.5S RNA gene (http://regulondb.ccg.unam.mx; Softberry, BPROM algorithm; http://www.softberry.com) gave predictions for transcription start points of σ^{70} RNA polymerase at positions –160, –130 and –26 relative to the mature 5′-end (nt +1) of 4.5S RNA. This corresponds to RNA-Seq reads with 5′-ends primarily at –26 and some with 5′-ends at about –153 and –127. However, at present the exact lengths of the 4.5S RNA precursor signals in Figure 2B remain unclear.

We further asked the question if the primer extension product for mature 4.5S RNA in BW[At*PRORP1*] further decreases after extended growth in glucose medium, and whether BW bacteria complemented with *At*PRORP1 or 3 differ in their 4.5S RNA processing defect. However, after ∼14 h (stationary phase) as well as following an additional outgrowth from stationary phase (in glucose medium), essentially no mature 4.5S RNA was detectable in BW[At*PRORP1*] as well as BW[At*PRORP3*] bacteria (Figure 2B, lanes 8–11).

Extended RNA-Seq analysis

To obtain statistically relevant data on tRNA processing defects in *E. coli* cells depending on PRORP isoenzymes, we performed a second RNA-Seq analysis based on three biological replicates. This included the strains BW[At*PRORP1*] and BW[At*PRORP3*] and *E. coli* BW[Ec*rnpB*] as reference strain for direct comparability with the results of our growth analysis (Figure 1). All cDNA reads of *E. coli* tRNAs were analyzed for their 5′-end position to evaluate cleavage site selection by the different RNase P enzymes. In the libraries of *E. coli* BW[Ec*rnpB*], BW[At*PRORP1*] and BW[At*PRORP3*], only tRNA reads starting either at the 5′-end position

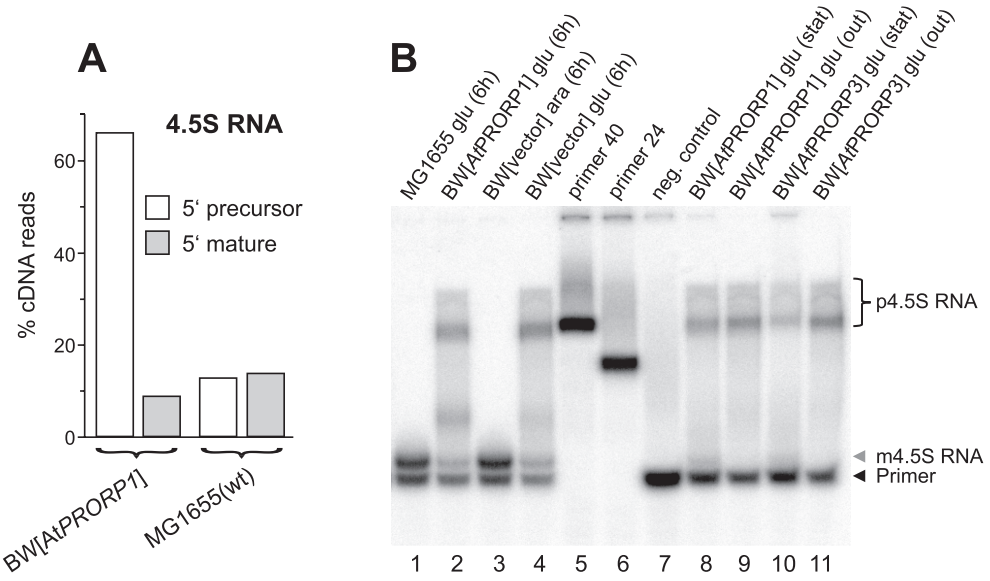

Figure 2. Processing of pre-4.5S RNA in *At*PRORP-depending *E. coli* cells. (**A**) Fraction of 5′-precursor and 5′-mature reads for *E. coli* 4.5S RNA in total RNAs derived from *E. coli* BW[At*PRORP1*] versus MG1655 wild type cells, determined by RNA-Seq (read alignment illustrated in Supplementary Figure S4). The remaining fraction (to 100%) were reads corresponding to internal 4.5S RNA fragments**.** Total RNAs were prepared after growth for 70 min in arabinose-free LB medium. For raw RNA-Seq data, see Online Supplement (http://bioinf.pharmazie.uni-marburg.de/supplements/prorp_2017/) under 'Initial Mapping'. (**B**) Identification of the 4.5S RNA 5′-ends by primer extension analysis. Total RNAs (30 μg) of *E. coli* strains grown for 6 h in the presence of glucose (glu) medium (*E. coli* MG1655, lane 1; *E. coli* BW[At*PRORP1*], lane 2; *E. coli* BW[pDG148(S/X)] (= BW[vector]), lane 4) or arabinose (ara) medium (*E. coli* BW[vector], lane 3) were used for reverse transcription with a 5′-^{32}P-end-labeled primer annealing to nt 20 to 3 of mature 4.5S RNA (m4.5S RNA). Total RNAs of *E. coli* BW[At*PRORP1*] (lane 8) and *E. coli* BW[At*PRORP3*] (lane 10) grown for ∼14 h in glucose medium (= stat, stationary phase), or further diluted in fresh glucose medium (starting OD_{600} ∼ 0.1) and growth for another ∼4 h to OD_{600} = 1.0 (= out, outgrowth from stationary phase; *E. coli* BW[At*PRORP1*], lane 9; *E. coli* BW[At*PRORP3*], lane 11), were analyzed in the same manner. As size markers we used 5′-^{32}P-end-labeled 44 nt (lane 6) and 60 nt (lane 5) long DNA oligonucleotides corresponding to cDNAs that would be obtained on pre-4.5S RNAs (p4.5S RNAs) with 24 and 40 nt long 5′-leaders, respectively; indicated as '(primer 40)' and '(primer 24)'. A primer extension reaction without RNA template served as negative control (lane 7). Extension products were analyzed by 20% denaturing PAGE.

–2, –1 or +1 were included in the evaluation (for details, see Materials and Methods). In Figure 3, the percentage of canonically processed cDNA reads (5′-end at nt +1) is plotted for all evaluated tRNAs (for read number cutoff, see Materials and Methods). Whereas cleavage site selection was overall similar in cDNA libraries derived from BW[Ec*rnpB*] and BW[At*PRORP3*] bacteria, our data suggested reduced processing at the canonical –1/+1 site for a set of tRNAs in BW[At*PRORP1*] (Figure 3). Generally, aberrant processing correlated well with the propensity of pre-tRNAs to form acceptor stems extended by one or two (N_{-1} : N_{+73}, N_{-2} : C_{+74}) base pairs (Supplementary Table S6): pre-tRNA Ser(CGA) can form an additional C_{-1} : G_{+73} pair, the three Asp(GUC) variants two extra G:C pairs or one G:U pair plus two G:C pairs, and pre-tRNAs Pro(GGG), Thr(GGU) 2/2, Val(UAC) 1/3 and Leu(GAG) can each form two extra pairs (U:A and G:C).

With the exception of some α-proteobacteria (24,25), all bacterial pre-tRNA^{His} species analyzed so far are cleaved by their cognate RNase P enzymes between nt –2 and –1 to release a mature functional tRNA^{His} with an 8-bp acceptor stem including the extra G_{-1} : C_{+73} base pair. This redirection of the cleavage site is caused by a combination of several structural determinants, as studied in depth for *E. coli* RNase P: a U at –2 and a G at –1 act as positive determinants for selection of the non-canonical –2/–1 site (26,27), and a G residue at –1 and a C at +73 (the discriminator) function as negative determinants for cleavage at the canonical –1/+1 site. The G_{-1} : C_{+73} base pair precludes interaction of C_{+73} with U_{294} (*E. coli* numbering) in the L15 loop of RNase P RNA, normally a mechanistic requirement for committing enzyme:substrate complexes to cleavage at the canonical –1/+1 site (28,29). In contrast to bacteria, pre-tRNA^{His} is canonically processed to a 5′-mature tRNA with a 7-bp acceptor stem in the eukaryotic nucleus/cytoplasm, and a G_{-1} residue is added by a tRNA^{His} guanylyltransferase (30,31). Recently, it was proposed that both, the bacterial and eukaryal, tRNA^{His} 5′-maturation pathways coexist in plant mitochondria (32). These findings suggested that 5′-processing of tRNA^{His} by *At*PRORP1 in *E. coli* BW bacteria might be ambiguous. RNA-Seq indeed revealed aberrant processing of tRNA^{His} by *At*PRORP1 (Figure 3). Whereas cDNA reads corresponding to a 5′-terminus at G_{+1} (corresponding to miscleavage at nt –1/+1) were negligible or only slightly increased in BW[Ec*rnpB*] and BW[At*PRORP3*], respectively, roughly half of the reads corresponded to miscleaved rather than correctly processed (5′-end at G_{-1}, cleavage at nt –2/–1) tRNA^{His} in BW[At*PRORP1*] cells (Figures 3 and 4A). We further analyzed by northern blotting if the overall levels of tRNA^{His} may be altered in BW[At*PRORP1*]. However, tRNA^{His} levels were equal in all tested strains grown in the presence of glucose (Figure 4B). Of note, the northern blot

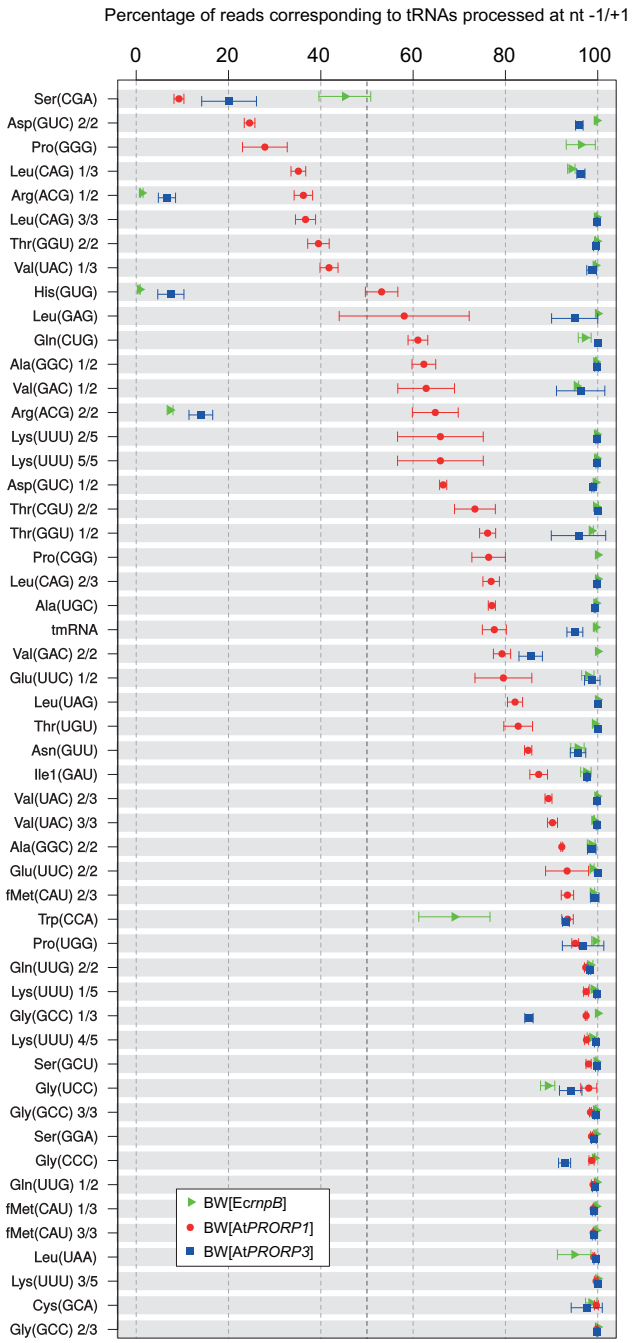

Figure 3. Percentage of tRNA reads corresponding to canonical cleavage between nt –1 and +1 (5′-end at position +1) in BW[Ec*rnpB*], BW[At*PRORP1*] and BW[At*PRORP3*] cells. Only tRNA reads with 5′-ends at position –2, –1 or +1 were included in the anaylsis (for details, see Material and Methods). Note that $tRNA^{His}$ is naturally miscleaved at nt –2/–1 (5′-end at nt –1) in bacteria, explaining why hardly any 5′-ends at position +1 were identified in BW[Ec*rnpB*] cells. RNA was prepared from cells outgrown from stationary to exponential growth phase ($OD_{600} \sim 0.7$) in arabinose-free LB medium and analyzed by RNA-Seq (three biological replicates of each strain).

signal of $tRNA^{His}$ derived from BW[At*PRORP1*] bacteria (Figure 4B, lane 3) reproducibly migrated slightly faster than the band from BW[At*PRORP3*] bacteria (Figure 4B, lane 4), in line with substantial aberrant processing at the –1/+1 site by *At*PRORP1 (Figure 3).

In Figure 3, the fraction of canonically processed $tRNA^{Arg}$(ACG) 1/2 and 2/2 appeared to be lower in BW[Ec*rnpB*] and BW[At*PRORP3*] than BW[At*PRORP1*] bacteria, although these pre-tRNAs have only the potential to form a weaker additional $U_{-1} : A_{+73}$ base pair (Supplementary Table S6). We have no plausible explanation for this finding.

Northern blot analyses of pre-$tRNA^{Sec}$ processing in *At*PRORP-dependent *E. coli* cells

Reads for $tRNA^{Sec}$, the second bacterial tRNA species containing an 8-bp acceptor stem generated by non-canonical 5′-end maturation (33), fell below the threshold for minimum read numbers and were thus not represented in Figure 3. Noteworthy, pre-$tRNA^{Sec}$ transcripts have the potential to extend their acceptor stems by two additional G:C base pairs, resulting in pre-tRNAs with a 10-bp acceptor stem (see Figure 5). We then analyzed $tRNA^{Sec}$ processing by northern blotting using total RNA from exponentially grown cells. We surprisingly observed a strong 5′-maturation defect in *E. coli* cells depending on *At*PRORP1 or *At*PRORP3 (Figure 4C, lanes 3 and 4). In BW[At*PRORP1*] bacteria mature $tRNA^{Sec}$ levels were largely decreased, while a precursor molecule accumulated (a 24-nt leader according to (33), 20–25 nt according to our RNA-Seq data). In BW[At*PRORP3*] cells grown in the presence of glucose, the pattern looked similar, but overall signal strength was largely diminished (Figure 4C, lane 4), suggesting that unprocessed $tRNA^{Sec}$ transcripts are degraded. In contrast, mature $tRNA^{Sec}$ was detected in *E. coli* BW[At*PRORP1*] and BW[At*PRORP3*] grown in medium supplemented with arabinose (Figure 4C, lanes 5 and 6). All total RNA preparations were quantitatively and qualitatively comparable as shown by the 5S RNA control (Figure 4*C*, bottom panel). Identical results were obtained with RNA preparations from stationary phase cells (data not shown).

In vitro cleavage of *E. coli* pre-$tRNA^{His}$, pre-$tRNA^{Sec}$ and pre-4.5S RNA by *At*PRORPs

To further substantiate the results of the *in vivo* analyses we investigated *in vitro* processing of 5′-^{32}P-end-labeled pre-$tRNA^{His}$, pre-$tRNA^{Sec}$ and the non-tRNA substrate 4.5S RNA by *At*PRORP1, 2 and 3 (Figure 5). As reference substrate we used pre-$tRNA^{Gly}$ from *Thermus thermophilus,* a standard class I tRNA (structurally very similar to its *E. coli* counterpart, but with slightly G:C-richer stem regions). Cleavage assays were performed under conditions of enzyme excess to exclude any rate limitations caused by product release (120 nM enzyme, <1 nM substrate) for 20 min at 28°C (*At*PRORP2) or 37°C (*At*PRORP1 and 3). In parallel, each substrate was incubated with the bacterial RNase P holoenzyme from *E. coli* under the same reaction conditions at 37°C. Whereas all three *At*PRORP enzymes

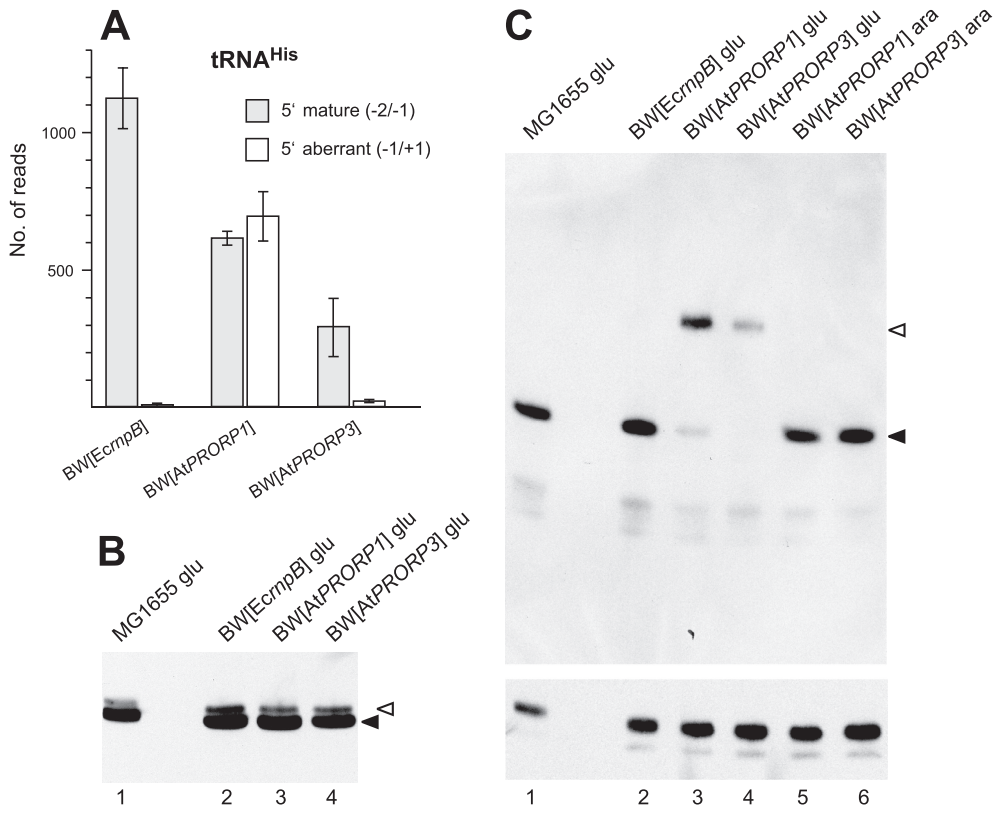

Figure 4. (**A**) Reads corresponding to $tRNA^{His}$ canonically processed at nt –2/–1 and aberrantly at nt –1/+1 in *E. coli* BW[Ec*rnpB*], BW[At*PRORP1*] and BW[At*PRORP3*] based on the RNA-Seq data presented in Figure 3. (B, C) Northern blot analysis of (**B**) $tRNA^{His}$ and (**C**) $tRNA^{Sec}$ levels in *E. coli* MG1655 (lanes 1), BW[Ec*rnpB*] (lanes 2), BW[At*PRORP1*] (lanes 3 and 5) and BW[At*PRORP3*] (lanes 4 and 6). Total RNA was prepared from outgrowth cultures grown until $OD_{600} \sim 1.0$ at 37°C in glucose-containing (lanes 1–4) or arabinose-containing (lanes 5 and 6) LB medium. After separation on 10% denaturing PAGE (9 μg RNA loaded per lane) the RNA was blotted onto a nylon membrane; $tRNA^{His}$ and $tRNA^{Sec}$ were hybridized with specific digoxigenin-labeled antisense RNA probes (for details, see Supplementary Table S4); signals indicated by filled arrowheads were assigned to mature $tRNA^{His}$ and $tRNA^{Sec}$, respectively, while signals marked by open arrowheads were interpreted as pre-tRNAs with a few nucleotides at the 5′- or 3′-end in the case of $tRNA^{His}$ and with long 5′-extensions in the case of $tRNA^{Sec}$. (**C**) After detection of $tRNA^{Sec}$ levels, the nylon membrane was treated with stripping solution and was reprobed with a 5S RNA (*rrfH*)-specific digoxigenin-labeled antisense RNA probe to control for RNA loading and quality (bottom panel).

processed pre-$tRNA^{Gly}$ efficiently and at the canonical site (Figure 5B, lanes 2–5), the other two tRNA substrates were cleaved unequally by the three *At*PRORP isoenzymes. Only *At*PRORP2 and 3 cleaved *E. coli* pre-$tRNA^{His}$ and pre-$tRNA^{Sec}$ preferentially at the bacteria-typical –2/–1 site producing a 9-nt and 14-nt 5′-flank, respectively (Figure 5B, lanes 8, 9, 13 and 14). With *At*PRORP1, both substrates were cleaved to >50% at the (for these tRNAs) aberrant –1/+1 site to generate non-functional $tRNA^{His}$ and $tRNA^{Sec}$ moieties (Figure 5B; lanes 7 and 12). Furthermore, all three, and particularly *At*PRORP2 and 3, cleaved pre-$tRNA^{Sec}$ less efficiently than pre-$tRNA^{Gly}$ and pre-$tRNA^{His}$, as suggested by the residual fraction of uncleaved substrate (Supplementary Table S7).

*At*PRORP1, 2 or 3 were unable to convert *E. coli* pre-4.5S RNA to its 5′-mature form (Figure 5B, lanes 17–19). In contrast, this non-tRNA substrate was processed by the bacterial RNase P holoenzyme from *E. coli* (Figure 5*B*, lanes 16). This finding is in line with the initial RNA-Seq and the primer extension data (Figure 2A and B).

Northern blot and primer extension analyses of other tRNAs in *At*PRORP-dependent *E. coli* cells

The Northern blot analysis was extended to $tRNA^{Ser}$(CGA) and $tRNA^{Asp}$(GUC) 2/2 (first and second row in Figure 3); for $tRNA^{Asp}$(GUC) 2/2, RNA-Seq indicated low levels of canonical cleavage in BW[At*PRORP1*] bacteria, for $tRNA^{Ser}$(CGA) lowest levels of canonical cleavage in the same strain but also reduced levels in the other strains (Figure 3). As controls, we used $tRNA^{Arg}$(CCU) as a tRNA with the potential to extend the acceptor stem by a single U:A bp (not presented in Figure 3 because of cDNA reads below the cutoff) and $tRNA^{Ile1}$(GAU) as an example for which the RNA-Seq results indicated predominantly canonical cleavage in all strains (Figure 3 and Supplementary Figure S5). In the case of $tRNA^{Ile1}$(GAU) and $tRNA^{Arg}$(CCU), Northern blot analysis did not reveal any evidence for precursor accumulation or aberrant processing (Supplementary Figure S5).

$tRNA^{Asp}$(GUC). *Escherichia coli* encodes three $tRNA^{Asp}$(GUC) genes, of which *aspT* and *aspU* have also

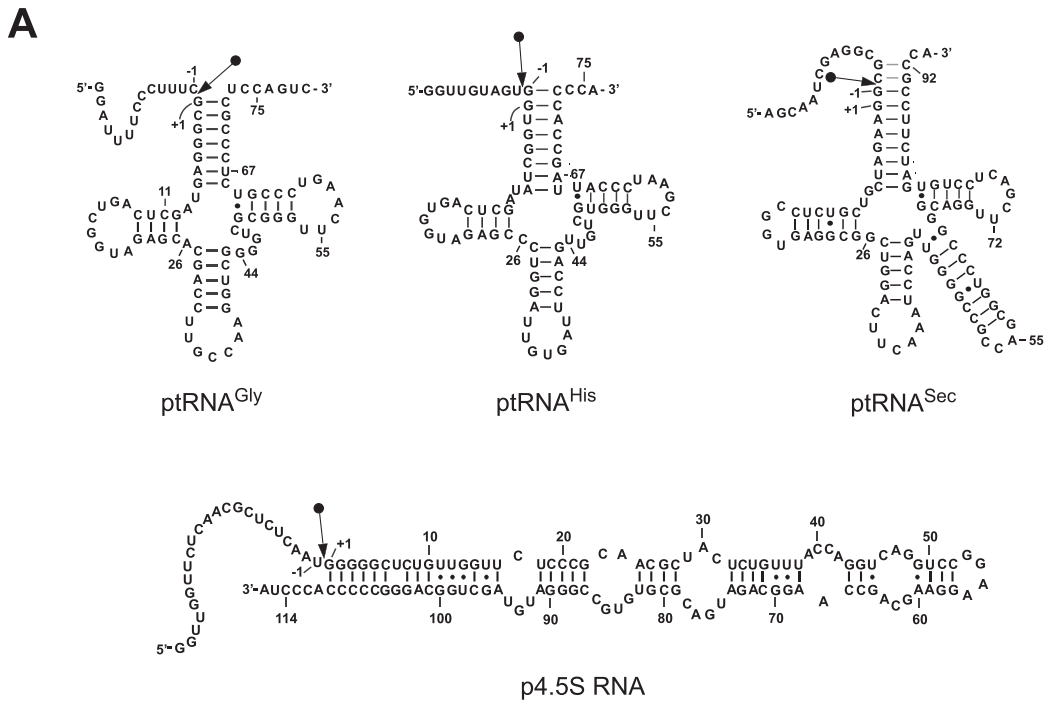

Figure 5. *In vitro* cleavage of canonical and non-canonical bacterial RNase P substrates by *E. coli* RNase P and *At*PRORP1, 2 and 3. (**A**) Substrate secondary structures. *T. thermophilus* pre-tRNA^{Gly} containing its natural 5′-flanking sequence (14 nt). *E. coli* pre-tRNA^{His} and pre-tRNA^{Sec} were equipped with a 5′-flanking sequence of 10 and 14 nt, respectively. The *E. coli* pre-4.5S RNA used here contained a 5′-flanking sequence of 23 nt. The canonical cleavage sites are marked by black arrows. (**B**) Cleavage of 5′-^{32}P-end labeled pre-tRNA^{Gly}, pre-tRNA^{His}, pre-tRNA^{Sec} and pre-4.5S RNA by *E. coli* RNase P (lanes 'Ec'; 100 nM RNase P RNA, 800 nM RNase P protein, 2 min incubation at 37°C), *At*PRORP1, 2 or 3 (lanes 'P1', 'P2' or 'P3', respectively; 120 nM enzyme, 20 min incubation at 37°C for *At*PRORP1 and 3, 20 min incubation at 28°C for *At*PRORP2); C, control (incubation of substrate for 20 min in the absence of enzyme). Canonical cleavage sites are marked by black, aberrant cleavage sites by gray arrowheads. Cleavage of pre-tRNA^{His} at site –1/+1 was quantified as 7.5 ± 1.1 (in %, ± standard deviation) for Ec, 63.7 ± 1.6 for P1, 9.7 ± 1.5 for P2 and 9.8 ± 1.9 for P3 (based on at least four independent experiments); cleavage of pre-tRNA^{Sec} at site –1/+1 was 6.1 ± 1.8 (in %, ± standard deviation) for Ec, 72.6 ± 3.6 for P1, 16.0 ± 2.8 for P2 and 12.4 ± 1.9 for P3 (based on at least 5 independent experiments). For more details on the cleavage assay, see the Supplementary Material.

identical 5′-leader sequences up to position –4 (Figure 6*A*); *aspT* and *aspU*, corresponding to Asp(GUC) 1/2 in Figure 3, can form a U_{-1} : G_{+73} wobble plus two extra G:C pairs, whereas *aspV* transcripts, corresponding to Asp(GUC) 2/2, have the potential to expand the acceptor stem by 2 G:C pairs (Figure 6A); *aspV* transcripts showed the strongest propensity of miscleavage in BW[At*PRORP1*] according to Figure 3. Elevated precursor levels were indeed observed in northern blots for $tRNA^{Asp}$(GUC) in BW[At*PRORP1*] cells (Figure 6B, lane 3), but hardly for BW[At*PRORP3*] cells (lane 4) and not at all for MG1655 and BW[Ec*rnpB*] bacteria (lanes 1 and 2). We also noticed that the main $tRNA^{Asp}$ band in RNA preparations from BW[At*PRORP1*] bacteria (Figure 6B, lane 3) migrated slightly slower than in the other lanes including the one representing BW[At*PRORP3*] cells (lane 4).

Since the resolution of the northern blots was relatively low, we further performed a primer extension analysis. Using RNA from exponentially grown cells (Figure 6*C*, outgrowth phase), we could confirm the northern blot results. In BW[At*PRORP1*] cells, little $tRNA^{Asp}$(GUC) cleaved at the canonical site was detected, but substantial amounts of tRNA processed at the aberrant –2/–1 site and precursor signals corresponding to 5′-extensions of about 6 to 8 nt. The latter extension products are consistent with 7-nt 5′-leader sequences seen in the RNA-Seq data of BW[At*PRORP1*] bacteria for $tRNA^{Asp}$(GUC) 1/2. In comparison, reduced but substantial amounts of $tRNA^{Asp}$(GUC) cleaved at the canonical site –1/+1 site were present in BW[At*PRORP3*] cells. In BW[At*PRORP3*], also signals for pre-tRNAs with about 7/8-nt long 5′-extensions were seen, and additionally signals representing longer precursors. Faint precursor signals were also detectable in RNA from MG1655 cells (Figure 6C, outgrowth phase). Interestingly, in stationary phase, levels of $tRNA^{Asp}$(GUC) precursors generally decreased and substantial amounts of canonically processed mature tRNA were now also present in RNA extracts from BW[At*PRORP1*] bacteria (Figure 6C, stationary phase).

$tRNA^{Ser}$(CGA). For $tRNA^{Ser}$(CGA), Northern blot experiments reproducibly detected a slightly reduced gel mobility of the main band in RNA extracts from BW[At*PRORP1*] bacteria (Figure 6B, lane 7), suggesting aberrant processing of *E. coli* $tRNA^{Ser}$(CGA) by *At*PRORP1, but not *At*PRORP3. Primer extension analysis confirmed that $tRNA^{Ser}$(CGA) transcripts are aberrantly processed at the –2/–1 site in BW[At*PRORP1*] bacteria, but evidently not in the BW[At*PRORP3*] strain (Figure 6D, outgrowth phase), for which the RNA-Seq data also suggested aberrant processing (Figure 3). In stationary phase, the fraction of correctly processed $tRNA^{Ser}$(CGA) again increased in BW[At*PRORP1*] cells, as seen for $tRNA^{Asp}$(GUC) (see above).

Complementation studies with other PRORPs and in *Bacillus subtilis*

*At*PRORP1 was unable to support growth of *B. subtilis* RNase P mutant bacteria (Supplementary Figure S6). Western blot analyses (Supplementary Figure S7) suggested that insolubility and degradation of *At*PRORP1 in *B. subtilis* are the major causes for the negative complementation results in this Gram-positive bacterium. Complementation by PRORP2 from *T. brucei* (*Tb*PRORP2) in our *E. coli* and *B. subtilis* RNase P mutant strains was found to be negative as well (Supplementary Figure S8), which is attributable to insolubility of the heterologous protein in the bacterial hosts (Supplementary Figure S9). In comparison, *At*PRORP1 was predominantly present in the soluble protein fraction of *E. coli* cells (Supplementary Figure S9C).

DISCUSSION

Processing of 4.5S RNA in *At*PRORP-depending *E. coli* cells

*At*PRORP1, 2 and 3 were not able to cleave 4.5S RNA *in vitro* under conditions where canonical tRNA substrates are processed efficiently. In accordance with this finding, RNA-Seq and primer extension analyses showed that 5′-precursor transcripts of 4.5S RNA accumulated in *E. coli* BW cells depending on *At*PRORP1 or 3. After prolonged growth of the *At*PRORP1 or 3 complementation strains, essentially no residual 5′-mature 4.5S RNA was detectable (Figure 2B, lanes 9 and 11). We thus conclude that *At*PRORP1 and 3 are essentially unable to contribute to 4.5S RNA 5′-end maturation in the *E. coli* host. This is in line with our previous finding that hairpin structures representing tRNA acceptor stem and T arm are poor substrates for *At*PRORP3 (34). Moreover, the 3′-terminal CCA is no crucial determinant for cleavage by *At*PRORP1 or *At*PRORP3 (34,35). Thus, we consider it unlikely that the 3′-CCC terminus of *E. coli* 4.5S RNA, which differs from the 3′-CCA end of tRNAs, might have contributed to the RNA's inability to be processed by PRORP enzymes. As 4.5S RNA is essential for cell survival (36) and BW[At*PRORP*] bacteria are viable despite the block of 4.5S RNA 5′-end maturation, our findings indicate that 4.5S RNA can exert its function in the presence of 5′-terminal extensions. Upon signal peptide exposure on the ribosome, the signal recognition particle (SRP), consisting of 4.5S RNA and protein Ffh, binds to the large ribosomal subunit where 4.5S RNA serves as a scaffold for the assembly of a complex between Ffh and the SRP receptor protein FtsY, and for relocation of the two proteins during the SRP membrane targeting cycle (37). A truncation of up to 10 bp from the distal end of 4.5S RNA was shown to be compatible with 4.5S RNA function in the SRP targeting cycle (37), suggesting that critical RNA-protein contacts are at some distance to the paired 5′- and 3′-ends. Thus, 4.5S RNA molecules with 5′-extensions are likely functional, in line with the viability of *At*PRORP-dependent *E. coli* cells devoid of detectable mature 4.5S RNA levels. Although we favor this interpretation, we cannot exclude the possibility that a small fraction of 5′-mature 4.5S RNA, not detected by primer extension in Figure 2*B*, is generated in BW[At*PRORP*] bacteria and maintains the essential function of the SRP, taking into account that the minimum number of 4.5S RNA molecules essential for growth of *E. coli* cells is unknown. A previous study showed that the number of 4.5S RNA molecules per

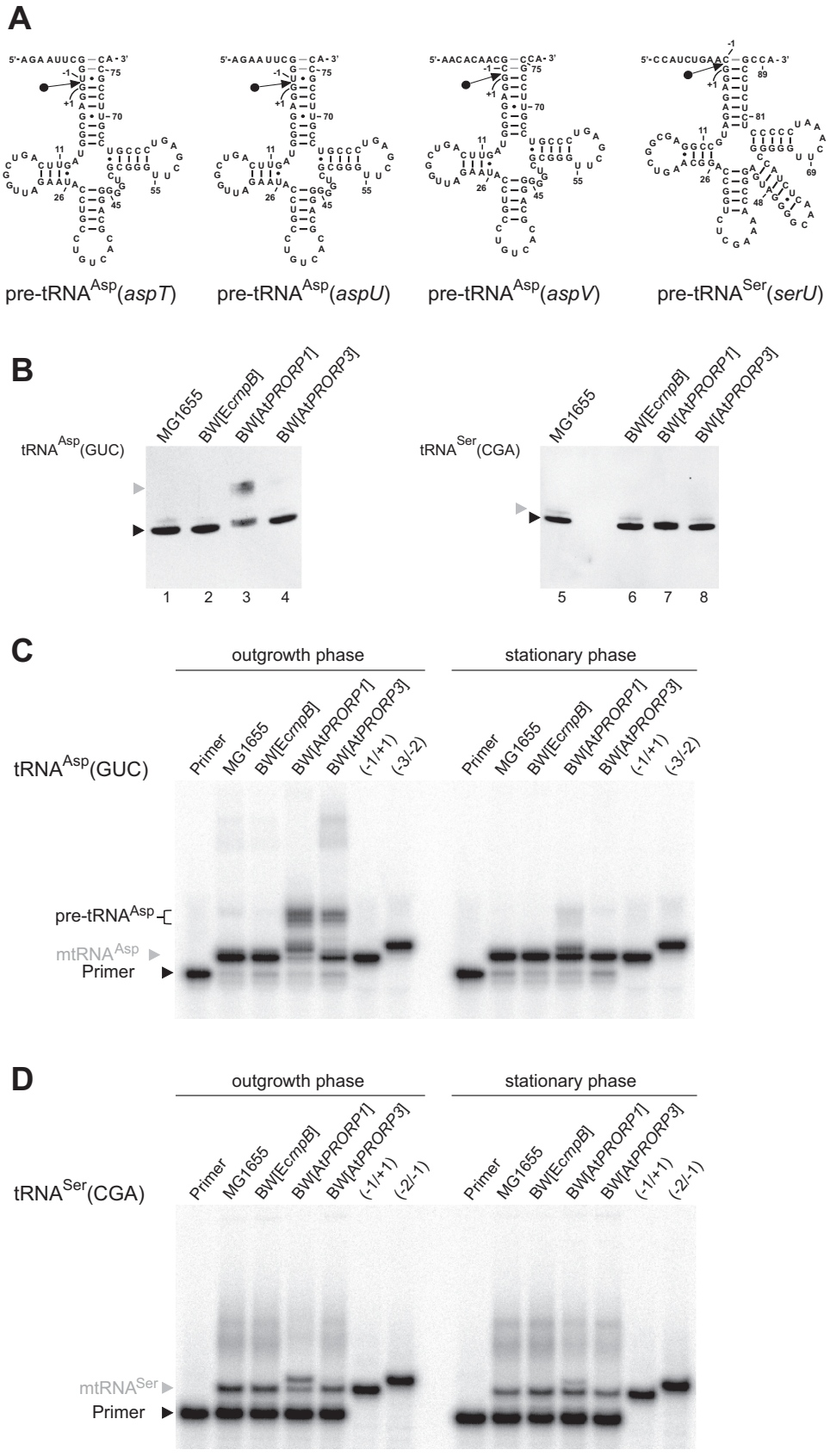

Figure 6. Processing of *E. coli* tRNAs^{Asp}(GUC) and tRNA^{Ser}(CGA) by *At*PRORP enzymes in *E. coli* BW. (**A**) Secondary structures of the analyzed *E. coli* precursor tRNAs encoded by *aspT*, *aspU*, *aspV* and *serU*; all four have the ability to form extended acceptor stem base pairings involving G:C base pairs.

E. coli MG1655 cell can vary between ∼450 and ∼5300 molecules in minimal versus rich media (38).

Processing of tRNA^{His} by *At*PRORP in *E. coli*

*At*PRORP1 miscleaves *E. coli* pre-tRNA^{His} *in vivo* and *in vitro* to a substantial extent (Figures 4*A* and 5). The absence of a G_{-1}, and thus the lack of the G_{-1} : C_{+73} bp, in *E. coli* RNA^{His} was shown to reduce aminoacylation efficiency by the cognate HisRS enzyme more than two orders of magnitude (39,40). Thus, at least half (Figure 5) of the tRNA^{His} processing products in *E. coli* BW[At*PRORP1*] bacteria are predicted to be non-functional. This may well have a negative effect on the protein synthesis rate, particularly affecting the translation of mRNAs enriched in histidine codons. We analyzed whether the cells may respond to the depletion of chargeable tRNA^{His} by increasing transcription from its single *hisR* gene, but northern blot analysis provided no evidence for elevated tRNA^{His} levels in BW[At*PRORP1*] bacteria grown in the presence of glucose (Figure 4B).

The finding that the nuclear *At*PRORP2 and 3 isoenzymes processed bacterial pre-tRNA^{His} at the –2/–1 site (34, this study) points to the previously noted flexibility of *At*PRORP3 to efficiently fit and process substrates extended by a single G:C base pair (34). As previously discussed, the biological significance of this feature is elusive and such acceptor stem extensions appear to be under negative selection in the nuclear tRNA genes of *A. thaliana* (34). Counterintuitively, *A. thaliana* mitochondria and chloroplasts encode bacterial-type tRNA^{His} genes (http://plantrna.ibmp.cnrs.fr/; (41)), however the organellar *At*PRORP1 cleaved only <50% of *E. coli* pre-tRNA^{His} at the upstream 'bacterial-like' site (–2/–1). These observations, although not understood at present, provide evidence that substrate recognition by organellar *At*PRORP1 is not identical to that of the nuclear isoenzymes.

Aberrant processing of tRNA^{Sec} by *At*PRORP1 in *E. coli*

Except for the American cranberry *Vaccinium macrocarpon* (42), genes for tRNA^{Sec} have not been found in flowering plants (41). Eukaryal tRNA^{Sec} molecules, if present, also differ from their bacterial counterparts in their acceptor and T stem structures (43). Thus, a bacterial-like tRNA^{Sec} is absent from the natural substrate spectrum of *At*PRORP enzymes. *E. coli* tRNA^{Sec}, encoded by the *selC* gene, carries a variable arm with more base pairs than in any other tRNA. Furthermore, it has an unusual D-arm with a 6-bp stem and a 4-nt loop. Nonetheless, bacterial tRNA^{Sec} assumes an L-shaped structure from which the long variable arm protrudes (44). TRNA^{Sec} is the second tRNA in *E. coli* beside tRNA^{His} that is subject to non-canonical processing by endogenous RNase P. 5′-End maturation leaves an 8-bp acceptor stem with an additional G_{-1} : C_{+73} bp as in tRNA^{His} (33). This is essential for incorporation of selenocysteine into three *E. coli* proteins, the formate dehydrogenases (Fdh) Fdh-O, Fdh-N and Fdh-H (45). The three Fdh proteins are involved in anaerobic energy metabolism, where they function in electron transfer from formate to nitrite *via* cytochrome c_{552} (46). However, other glycolysis metabolites (NADH, and possibly lactate and ethanol) can also mediate nitrite reduction (46). Considering that *E. coli* cells depending on *At*PRORP1 or *At*PRORP3 were (almost) devoid of mature tRNA^{Sec} (Figure 4*C*; BW[At*PRORP3*] even more than BW[At*PRORP1*] bacteria; lane 4 versus 3), this defect can be excluded as a reason for the slower growth of BW[At*PRORP1*] relative to BW[At*PRORP3*] cells (Figure 1).

The reduction of precursor and mature tRNA^{Sec} levels in BW[At*PRORP1*] and BW[At*PRORP3*] cells grown under non-permissive conditions can be explained by degradation of unprocessed precursor, and inefficient processing of pre-tRNA^{Sec} by *At*PRORP1 and 3 is attributable to the potential of this precursor to form an acceptor stem extended by three G:C base pairs (Figure 5A). Such G:C-rich extensions are not found in precursor tRNAs of *A. thaliana* (34), indicating that *At*PRORP enzymes have not been under evolutionary pressure to cope with such substrates. This is also in line with the *in vitro* processing results, demonstrating less efficient *At*PRORP processing of pre-tRNA^{Sec} relative to pre-tRNA^{His} and pre-tRNA^{Gly} in particular (Supplementary Table S7). We assign the observation of some *At*PRORP-catalyzed processing of pre-tRNA^{Sec} *in vitro*, but barely in *E. coli* cells, to the use of enzyme excess in the *in vitro* experiments. As observed for pre-tRNA^{His}, *At*PRORP1 had a higher propensity than the two other isoenzymes to cleave pre-tRNA^{Sec} *in vitro* at the (in this case) aberrant –1/+1 site.

PRORP isoenzyme-dependent complementation efficacy

Here, we have shown that all three PRORP isoenzymes from *A. thaliana* are able to support growth of *E. coli* mutant bacteria in rich medium under conditions where endogenous RNase P levels are insufficient to sustain

←

Ten 5′-leader nucleotides are arbitrarily shown for each tRNA. Black arrows mark the canonical cleavage sites between nt –1 and +1. (**B**) Northern blot detection of tRNA^{Asp}(GUC) and tRNA^{Ser}(CGA). Total cellular RNA was isolated from exponential phase cultures (at OD_{600} ∼ 1.0) grown in glucose medium (see Suppl. Material for details). Mature tRNAs and presumptive 5′-precursor tRNAs are indicated by black and gray arrowheads, respectively. (**C**, **D**) Identification of the 5′-ends of tRNA^{Asp}(GUC) and tRNA^{Ser}(CGA) in *E. coli* MG1655, BW[E*crnpB*], BW[At*PRORP1*] and BW[At*PRORP3*] by primer extension analysis. For total RNA preparation cell cultures were grown overnight to stationary phase in LB medium supplemented with glucose (OD_{600} ∼ 6.7 to 10.6, right panels). In addition, aliquots of the stationary cultures were diluted in fresh glucose medium (starting OD_{600} ∼ 0.1) and further grown to OD_{600} = 1.0 (outgrowth from stationary phase, left panels) before RNA preparation. For details of primer extension, see the Supplementary Material. 5′-^{32}P-end-labeled DNA oligonucleotides, 22 and 24 nt long and corresponding to cDNAs that would be obtained on correctly (+1/–1) and aberrantly (–2/–3) cleaved tRNA^{Asp}, served as size markers (panel C). Based on these size markers, aberrant cleavage of tRNA^{Asp}(GUC) in BW[At*PRORP1*] cells was assigned to –2/–1. In panel D, 5′-^{32}P-end-labeled DNA oligonucleotides, 22 and 23 nt long and corresponding to cDNAs that would be obtained on correctly (+1/–1) and aberrantly (–1/–2) cleaved tRNA^{Ser}, served as size markers; pre-tRNA^{Asp}, precursor of tRNA^{Asp}; mtRNA^{Asp} and mtRNA^{Ser}, mature tRNA^{Asp} and tRNA^{Ser}, respectively; *Primer*, 5′-^{32}P-end-labeled DNA oligonucleotide used for the respective primer extension analysis.

growth. Thus, all three protein enzymes can take over basic and essential functions in tRNA 5′-end maturation normally catalyzed by the endogenous RNP enzyme. Surprisingly, *E. coli* bacteria depending on *At*PRORP3 reproducibly showed a shorter lag phase than those complemented with *At*PRORP1 (Figure 1). 4.5S RNA primer extension data (Figure 2) and northern blot results revealed that both isoenzymes are unable to process pre-4.5S RNA molecules and are largely deficient in $tRNA^{Sec}$ maturation (*At*PRORP3 even more than *At*PRORP1; Figure 4) precursor molecules. Thus, the 4.5S RNA and $tRNA^{Sec}$ processing defects cannot be the reason for the shorter lag phase of the BW[At*PRORP3*] strain. However, for several tRNAs our RNA-Seq analysis revealed increased levels of aberrant cleavage in BW[*At*PRORP1]. For selected tRNAs we were able to validate the RNA-Seq data in a more detailed biochemical analysis. For example, *At*PRORP3 cleaved $tRNA^{His}$ at the functional -2/-1 site, whereas *At*PRORP1 selected this cleavage site to 50% or less (Figures 3 and 5). Also, the retardation of $tRNA^{Asp}$(GUC) processing was more pronounced in *E. coli* cells depending on *At*PRORP1 relative to *At*PRORP3 activity (Figure 6B and C). Likewise, aberrant processing of $tRNA^{Asp}$(GUC) and $tRNA^{Ser}$(CGA) 1 nt upstream of the canonical site was only observed in the *At*PRORP1 complementation strain (Figure 6C and D). Generally, aberrant processing by *At*PRORP1 correlated well with pre-tRNA acceptor stem extensions involving G:C base pairs (Supplementary Table S6). These differences provide a straightforward explanation for the shorter lag phase of BW[At*PRORP3*] relative to BW[At*PRORP1*] bacteria (Figure 1). Interestingly, the $tRNA^{Asp}$(GUC) and $tRNA^{Ser}$(CGA) processing defects in BW[At*PRORP1*] bacteria were more pronounced in exponential than stationary phase (Figure 6C and D). This suggests that *At*PRORP1 catches up with processing of these tRNAs in stationary phase when global transcription slows down and cell division stops, apparently by re-processing of aberrantly processed tRNAs.

The molecular basis for deviant substrate recognition by *At*PRORP1 versus *At*PRORP3 in *E. coli* cells remains to be investigated. Western blot analysis (Supplementary Figure S3) suggested that expression levels and solubility of the two isoenzymes are comparable. Thus, we cautiously conclude that solubility differences between *At*PRORP1 and 3 in *E. coli* were likely not relevant to the observed growth difference. However, this conclusion does not apply to other complementation setups, as unsuccessful complementation of *At*PRORP1 in *B. subtilis* RNase P mutant bacteria (Supplementary Figure S6) and of *Tb*PRORP2 in *E. coli* and *B. subtilis* (Supplementary Figure S8) could be attributed to insolubility and fragmentation of *At*PRORP1 in the *B. subtilis* host (Supplementary Figure S7) and pronounced insolubility of *Tb*PRORP2 in *E. coli* and *B. subtilis* (Supplementary Figure S9).

Maturation of $tRNA^{His}$ in different biological systems

The present study revealed that *At*PRORP2/3 enzymes, like bacterial RNA-based RNase P enzymes, have the capacity to fully shift the cleavage site to nt –2/–1 when acting on pre-$tRNA^{His}$ carrying an extra $G_{-1} : C_{+73}$ base pair. In Eukarya, the G_{-1}, not encoded in $tRNA^{His}$ genes, is added by $tRNA^{His}$ guanylyltransferase (THG1) after RNase P processing. In those Archaea, where G_{-1} is genomically encoded, the RNase P enzymes (one RNA plus five protein cofactors) are thought to be still able to switch the cleavage site on pre-$tRNA^{His}$. However, in other Archaea with G_{-1} not encoded in the $tRNA^{His}$ gene, the G_{-1} has to be added by the respective THG1 enzyme (47). For *A. thaliana* mitochondria, it has been proposed that both the bacterial and the eukaryal nuclear RNP 5′-maturation pathways for $tRNA^{His}$ coexist (32). The presence of the eukaryal pathway was inferred from two lines of evidence: (i) expression of larch pre-$tRNA^{His}$ lacking G_{-1} in potato mitochondria and the subsequent identification of larch $tRNA^{His}$ molecules with G_{-1} added post-transcriptionally; (ii) transfer of a radioactive G_{-1} residue onto a 5′-G_{+1}-$tRNA^{His}$ by a guanylyltransferase activity in potato mitochondrial extracts; the identity of the enzyme remained unclear and was shown to be different from the two *A. thaliana* THG1 homologs that localize to the nucleoplasm (32). Whatever the identity of this mitochondrial guanylyltransferase activity is, it seems to be quite inefficient, as substantial steady-state levels of non-functional $tRNA^{His}$ molecules lacking G_{-1} are detectable in the mitochondria of potato plants grown under normal conditions. Apparently, plant mitochondria tolerate the presence of a substantial fraction of inactive $tRNA^{His}$ molecules (with 5′-G_{+1}) derived from imprecise pre-$tRNA^{His}$ processing by *At*PRORP1. The presence of non-aminoacylated $tRNA^{His}$ resulting from ambiguous 5′-end maturation may also hint at a novel and so far unknown regulatory function in plant mitochondria.

Evolutionary implications

Catalytic RNA-based bacterial RNase P and PRORP enzymes are apparently the result of convergent evolution. The core task of both is the 5′-end maturation of canonical tRNAs, whose structures have remained essentially unchanged throughout evolution. However, the two types of RNase P differ in terms of specificity for substrates that deviate from canonical tRNA structures. *E. coli* RNase P, but not PRORP, can act efficiently on hairpin-like substrates. This is demonstrated in the present study for 4.5S RNA, a long-known non-tRNA substrate of *E. coli* RNase P (20,21), and is also suggested for structurally related substrates including phage ϕ80-induced M3 RNA (48), CI RNA from satellite phage P4 (49), the C4 repressor RNA of bacteriophages P1/P7 (50) and some other *E. coli* RNAs (for a review, see (1)). Those substrates lack a T loop equivalent, one of the most conserved tRNA features. The capacity of bacterial RNase P to specifically act on minimalistic substrates, originally discovered by Altman and coworkers (51,52), can be attributed to the enzyme's recognition of multiple elements near the cleavage site, including the base pairing interaction between substrate 3′-ends and the L15 loop of RNase P RNAs, as well as selective binding of unstructured 5′-precursor segments through the bacterial RNase P protein. For PRORP enzymes, the only natural, non-canonical substrates

known so far are so-called t-elements (53). T-elements are associated with 5′- or 3′-termini of several plant mitochondrial mRNAs and appear to act as *cis*-signals for endonucleolytic cleavages by RNase P and/or RNase Z (54). T-elements look like degenerated tRNAs, harboring acceptor stem/T-arm mimics but lacking the anticodon arm (*A. thaliana nad6*) or a canonical D arm (*Brassica napus orf138*) (9,10,54). However, with their conservation of T loop and the presence of at least a degenerated D arm, t-elements are structurally more closely related to canonical tRNAs than extended hairpin substrates such as 4.5S RNA. In addition, our study has revealed that the organellar *At*PRORP1 enzyme has difficulties to act on pre-tRNAs that can form acceptor stem extensions involving G:C base pairs. *At*PRORP3 was less sensitive to such extensions, but failed on pre-tRNA^{Sec} with its acceptor stem expanded by three G:C pairs, again consistent with previously reported findings on cleavage-site selection by *At*PRORP3 (34). Future studies will have to address the molecular basis for the differences we have observed here between *At*PRORP1 and *At*PRORP3. Despite these differences between isoenzymes, it appears that PRORPs, like nuclear RNP RNase P enzymes (55–57), use different, structure- rather than sequence-based mechanisms of substrate recognition and cleavage site selection (34) and, as a result, PRORPs have a narrower, more canonical tRNA-centric substrate spectrum than bacterial RNase P enzymes.

SUPPLEMENTARY DATA

Supplementary Data are available at NAR Online.

ACKNOWLEDGEMENTS

We like to thank Michael E. Harris for providing us with plasmid pEc595, Manja Marz for initial help with RNA-Seq data processing and Clemens Thölken for bioinformatic support.

FUNDING

German Research Foundation (DFG) [HA 1672/17-1 to R.K.H., IRTG 1384 to M.L., R.K.H.]; Austrian Science Fund (FWF) [I299 to W.R.]. Funding for open access charge: state money, grants.
Conflict of interest statement. None declared.

REFERENCES

1. Hartmann,R.K., Gößringer,M., Späth,B., Fischer,S. and Marchfelder,A. (2009) The making of tRNAs and more - RNase P and tRNase Z. *Prog. Mol. Biol. Transl. Sci.*, **85**, 319–368.
2. Lai,L.B., Vioque,A., Kirsebom,L.A. and Gopalan,V. (2010) Unexpected diversity of RNase P, an ancient tRNA processing enzyme: challenges and prospects. *FEBS Lett.*, **584**, 287–296.
3. Liu,F. and Altman,S. (eds). (2010) *Ribonuclease P*. Springer, NY.
4. Esakova,O. and Krasilnikov,A.S. (2010) Of proteins and RNA: the RNase P/MRP family. *RNA*, **16**, 1725–1747.
5. Guerrier-Takada,C., Gardiner,K., Marsh,T., Pace,N and Altman,S. (1983). The RNA moiety of ribonuclease P is the catalytic subunit of the enzyme. *Cell*, **35**, 849–857.
6. Hartmann,E. and Hartmann,R.K. (2003) The enigma of ribonuclease P evolution. *Trends Genet.*, **19**, 561–569.
7. Walker,S.C. and Engelke,D.R. (2006) Ribonuclease P: the evolution of an ancient RNA enzyme. *Crit. Rev. Biochem. Mol. Biol.*, **41**, 77–102.
8. Holzmann,J., Frank,P., Löffler,E., Bennett,K.L., Gerner,C. and Rossmanith,W. (2008) RNase P without RNA: identification and functional reconstitution of the human mitochondrial tRNA processing enzyme. *Cell*, **135**, 462–474.
9. Gobert,A., Gutmann,B., Taschner,A., Gößringer,M., Holzmann,J., Hartmann,R.K., Rossmanith,W. and Giegé,P. (2010) A single *Arabidopsis* organellar protein has RNase P activity. *Nat. Struct. Mol. Biol.*, **17**, 740–744.
10. Gutmann,B., Gobert,A. and Giegé,P. (2012) PRORP proteins support RNase P activity in both organelles and the nucleus in *Arabidopsis*. *Genes Dev.*, **26**, 1022–1027.
11. Taschner,A., Weber,C., Buzet,A., Hartmann,R.K., Hartig,A. and Rossmanith,W. (2012) Nuclear RNase P of *Trypanosoma brucei*: a single protein in place of the multicomponent RNA-protein complex. *Cell Rep.*, **2**, 19–25.
12. Weber,C., Hartig,A., Hartmann,R.K. and Rossmanith,W. (2014) Playing RNase P evolution: swapping the RNA catalyst for a protein reveals functional uniformity of highly divergent enzyme forms. *PLoS Genet.*, **10**, e1004506.
13. Howard,M.J., Karasik,A., Klemm,B.P., Mei,C., Shanmuganathan,A., Fierke,C.A. and Koutmos,M. (2016) Differential substrate recognition by isozymes of plant protein-only Ribonuclease P. *RNA* **22**, 782–792.
14. Wegscheid,B. and Hartmann,R.K. (2006) The precursor tRNA 3′-CCA interaction with *Escherichia coli* RNase P RNA is essential for catalysis by RNase P *in vivo*. *RNA*, **12**, 2135–2148.
15. Damm,K., Bach,S., Müller,K.M., Klug,G., Burenina,O.Y., Kubareva,E.A., Grünweller,A. and Hartmann,R.K. (2015) Impact of RNA isolation protocols on RNA detection by Northern blotting. *Methods Mol. Biol.*, **1296**, 29–38.
16. Hoffmann,S., Otto,C., Kurtz,S., Sharma,C.M., Khaitovich,P., Vogel,J., Stadler,P.F. and Hackermüller,J. (2009) Fast mapping of short sequences with mismatches, insertions and deletions using index structures. *PLoS Comput. Biol.*, **5**, e1000502.
17. Suzuki,T. and Miyauchi,K. (2010) Discovery and characterization of tRNA^{Ile} lysidine synthetase (TilS). *FEBS Lett.*, **584**, 272–277.
18. Dong,H., Nilsson,L. and Kurland,C.G. (1996) Co-variation of tRNA abundance and codon usage in *Escherichia coli* at different growth rates. *J. Mol. Biol.*, **260**, 649–663.
19. Pavlova,L.V., Gößringer,M., Weber,C., Buzet,A., Rossmanith,W. and Hartmann,R.K. (2012) tRNA processing by protein-only versus RNA-based RNase P: kinetic analysis reveals mechanistic differences. *Chembiochem.*, **13**, 2270–2276.
20. Bothwell,A.L., Garber,R.L. and Altman,S. (1976) Nucleotide sequence and *in vitro* processing of a precursor molecule to *Escherichia coli* 4.5 S RNA. *J. Biol. Chem.*, **251**, 7709–7716.
21. Peck-Miller,K.A. and Altman,S. (1991) Kinetics of the processing of the precursor to 4.5 S RNA, a naturally occurring substrate for RNase P from *Escherichia coli*. *J. Mol. Biol.*, **221**, 1–5.
22. Herskovits,A.A., Bochkareva,E.S and Bibi,E. (2000) New prospects in studying the bacterial recognition particle pathway. *Mol. Microbiol.* **38**, 927–939.
23. Ulbrandt,N.D., Newitt,J.A. and Bernstein,H.D. (1997) The *E. coli* signal recognition particle is required for the insertion of a subset of inner membrane proteins. *Cell* **88**,187–196.
24. Ardell,D.H. and Andersson,S.G. (2006) TFAM detects co-evolution of tRNA identity rules with lateral transfer of histidyl-tRNA synthetase. *Nucleic Acids Res.*, **34**, 893–904.
25. Wang,C., Sobral,B.W. and Williams,K.P. (2007) Loss of a universal tRNA feature. *J. Bacteriol.*, **189**, 1954–1962.
26. Brännvall,M., Fredrik Pettersson,B.M. and Kirsebom,L.A. (2002) The residue immediately upstream of the RNase P cleavage site is a positive determinant. *Biochimie*, **84**, 693–703.
27. Kikovska,E., Brännvall,M. and Kirsebom,L.A. (2006) The exocyclic amine at the RNase P cleavage site contributes to substrate binding and catalysis. *J. Mol. Biol.*, **359**, 572–584.
28. Kirsebom,L.A. (2002) RNase P RNA-mediated catalysis. *Biochem. Soc. Trans.*, **30**, 1153–1158.
29. Brännvall,M., Pettersson,B.M. and Kirsebom,L.A. (2003) Importance of the +73/294 interaction in *Escherichia coli* RNase P

RNA substrate complexes for cleavage and metal ion coordination. *J. Mol. Biol.*, **325**, 697–709.
30. Cooley,L., Appel,B. and Söll,D. (1982) Post-transcriptional nucleotide addition is responsible for the formation of the 5′ terminus of histidine tRNA. *Proc. Natl. Acad. Sci. U.S.A.*, **79**, 6475–6479.
31. Gu,W., Hurto,R.L., Hopper,A.K., Grayhack,E.J. and Phizicky,E.M. (2005) Depletion of *Saccharomyces cerevisiae* $tRNA^{His}$ guanylyltransferase Thg1p leads to uncharged $tRNA^{His}$ with additional m^5C. *Mol. Cell. Biol.*, **25**, 8191–8201.
32. Placido,A., Sieber,F., Gobert,A., Gallerani,R., Giegé,P. and Maréchal-Drouard,L. (2010) Plant mitochondria use two pathways for the biogenesis of $tRNA^{His}$. *Nucleic Acids Res.*, **38**, 7711–7717.
33. Burkard,U. and Söll,D. (1988) The unusually long amino acid acceptor stem of *Escherichia coli* selenocysteine tRNA results from abnormal cleavage by RNase P. *Nucleic Acids Res.*, **16**, 11617–11624.
34. Brillante,N., Gößringer,M., Lindenhofer,D., Toth,U., Rossmanith,W. and Hartmann,R.K. (2016) Substrate recognition and cleavage-site selection by a single-subunit protein-only RNase P. *Nucleic Acids Res.*, **44**, 2323–2336.
35. Mao,G., Chen,T.H., Srivastaval,A.S., Kosek,D., Biswas,P.K., Gopalan,V. and Kirsebom,L.A. (2016) Cleavage of model substrates by *Arabidopsis thaliana* PRORP1 reveals new insights into its substrate requirements. *PLoS One* **11**, e0160246.
36. Brown,S. and Fournier,M.J. (1984) The 4.5 S RNA gene of *Escherichia coli* is essential for cell growth. *J. Mol. Biol.*, **178**, 533–550.
37. Ataide,S.F., Schmitz,N., Shen,K., Ke,A., Shan,S.O., Doudna,J.A. and Ban,N. (2011) The crystal structure of the signal recognition particle in complex with its receptor. *Science*, **331**, 881–886.
38. Dong,H., Kirsebom,L.A. and Nilsson,L. (1996) Growth rate regulation of 4.5 S RNA and M1 RNA the catalytic subunit of *Escherichia coli* RNase P. *J. Mol. Biol.*, **261**, 303–308.
39. Himeno,H., Hasegawa,T., Ueda,T., Watanabe,K., Miura,K. and Shimizu,M. (1989) Role of the extra G-C pair at the end of the acceptor stem of $tRNA^{His}$ in aminoacylation. *Nucleic Acids Res.*, **17**, 7855–7863.
40. Connolly,S.A., Rosen,A.E., Musier-Forsyth,K. and Francklyn,C.S. (2004) G-1:C73 recognition by an arginine cluster in the active site of *Escherichia coli* histidyl-tRNA synthetase. *Biochemistry*, **43**, 962–969.
41. Cognat,V., Pawlak,G., Duchêne,A.M., Daujat,M., Gigant,A., Salinas,T., Michaud,M., Gutmann,B., Giegé,P., Gobert,A. and Maréchal-Drouard,L. (2013) PlantRNA, a database for tRNAs of photosynthetic eukaryotes. *Nucleic Acids Res.*, **41** , D273–D279.
42. Fajardo,D., Schlautman,B., Steffan,S., Polashock,J., Vorsa,N. and Zalapa,J. (2014) The American cranberry mitochondrial genome reveals the presence of selenocysteine (tRNA-Sec and SECIS) insertion machinery in land plants. *Gene*, **536**, 336–343.
43. Mizutani,T. and Goto,C. (2000) Eukaryotic selenocysteine tRNA has the 9/4 secondary structure. *FEBS Lett.*, **466**, 359–362.
44. Itoh,Y., Sekine,S., Suetsugu,S. and Yokoyama,S. (2013) Tertiary structure of bacterial selenocysteine tRNA. *Nucleic Acids Res.*, **41**, 6729–6738.
45. Sawers,G., Heider,J., Zehelein,E. and Böck,A. (1991) Expression and operon structure of the *sel* genes of *Escherichia coli* and identification of a third selenium-containing formate dehydrogenase isoenzyme. *J. Bacteriol.*, **173**, 4983–4993.
46. Darwin,A., Tormay,P., Page,L., Griffiths,L. and Cole,J. (1993) Identification of the formate dehydrogenases and genetic determinants of formate-dependent nitrite reduction by *Escherichia coli* K12. *J. Gen. Microbiol.*, **139**, 1829–1840.
47. Heinemann,I.U., Nakamura,A., O'Donoghue,P., Eiler,D. and Söll,D. (2012) $tRNA^{His}$-guanylyltransferase establishes $tRNA^{His}$ identity. *Nucleic Acids Res.*, **40**, 333–344.
48. Bothwell,A.L., Stark,B.C. and Altman,S. (1976) Ribonuclease P substrate specificity: Cleavage of a bacteriophage phi80-induced RNA. *Proc. Natl. Acad. Sci. U.S.A.*, **73**, 1912–1906.
49. Forti,F., Sabbattini,P., Sironi,G., Zangrossi,S., Deho,G. and Ghisotti,D. (1995) Immunity determinant of phage–plasmid P4 is a short processed RNA. *J. Mol. Biol.*, **249**, 869–878.
50. Hartmann,R.K., Heinrich,J., Schlegl,J. and Schuster,H. (1995) Precursor of C4 antisense RNA of bacteriophages P1 and P7 is a substrate for RNase P of *Escherichia coli*. *Proc. Natl. Acad. Sci. U.S.A.*, **92**, 5822–5826.
51. McClain,W.H., Guerrier-Takada,C. and Altman,S. (1987) Model substrates for an RNA enzyme. *Science*, **238**, 527–530.
52. Forster,A.C. and Altman,S. (1990) External guide sequences for an RNA enzyme. *Science*, **249**, 783–786.
53. Hanic-Joyce,P.J., Spencer,D.F. and Gray,M.W. (1990) *In vitro* processing of transcripts containing novel tRNA-like sequences ('t-elements') encoded by wheat mitochondrial DNA. *Plant Mol. Biol.*, **15**, 551–559.
54. Forner,J., Weber,B., Thuss,S., Wildum,S. and Binder,S. (2007) Mapping of mitochondrial mRNA termini in *Arabidopsis thaliana*: t-elements contribute to 5′ and 3′ end formation. *Nucleic Acids Res.*, **35**, 3676–3692.
55. Carrara,G., Calandra,P., Fruscoloni,P. and Tocchini-Valentini,G.P. (1995) Two helices plus a linker: a small model substrate for eukaryotic RNase P. *Proc. Natl. Acad. Sci. U.S.A.* **92**, 2627–2631.
56. Yuan,Y. and Altman,S. (1995) Substrate recognition by human RNase P: identification of small, model substrates for the enzyme. *EMBO J.*, **14**, 159–168.
57. Carrara,G., Calandra,P., Fruscoloni,P., Doria,M. and Tocchini-Valentini,G.P. (1989) Site selection by *Xenopus laevis* RNAase P. *Cell*, **58**, 37–45.